Understanding Error Generation in Fused Deposition Modeling

Cindy Bayley[1], Lennart Bochmann[3], Colin Hurlbut[2], Moneer Helu[1],
Robert Transchel[3], and David Dornfeld[1]

[1]Laboratory for Manufacturing and Sustainability
University of California, Berkeley
Berkeley, California, United States

[2]Department of Mechanical Engineering
University of California, Berkeley
Berkeley, California, United States

[3]Institute of Machine Tools and Manufacturing
Swiss Federal Institute of Technology Zurich
Zurich, Zurich, Switzerland

INTRODUCTION

Additive Manufacturing (AM) can improve flexibility and convenience, lower manufacturing costs, and reduce time to market for many manufacturing applications [1,2]. Successfully implementing and expanding AM requires improvements in surface quality, shear and tensile strength, build time, accuracy, and precision of these processes [3]. Of these issues, surface quality, accuracy, and precision are the biggest obstacles preventing AM from becoming a primary production process [4]. This paper aims to understand the relationship between process characterisitics and error generation in Fused Deposition Modeling (FDM), which is an AM process typically used for prototyping. Understanding error generation can improve the scalability of AM technologies and expand their use to create better products.

BACKGROUND

The major sources of error in the positional accuracy of the drop deposition of rapid prototyping systems, such as FDM, include mathematical errors due to the approximation of part surfaces in the standard file input; process-related errors such as positioning errors in the *xy* plane due to translation of the printer head and in the *z*-axis due to the registration of different layers; and material-related errors, such as shrinkage, distortion, and seepage of binder during production [5]. The accuracy of the printing process also depends on errors generated by each machine component. This paper primarily focuses on examining process- and machine-related errors.

The process characteristics that limit the accuracy of AM techniques, such as FDM, include the layer thickness, build orientation, raster angle, air gap, and raster width [3,5]. Of these, the build orientation has been found to be a primarily influence on the dimensional accuracy, surface roughness, shear and tensile strength, build time, required support structures, and cost of FDM parts [4,6]. The layer thickness and overlap interval between fibers also affects the surface roughness of printed parts [7]. This effect is due to the “staircase effect” in FDM processes. When FDM machines deposit beads of material layer by layer, a staircase-like structure is formed on inclined or rounded features, which increases surface roughness.

Examining the effect of FDM process parameters on part quality has been primarily accomplished using developed control parts. Clemon et al. [8] measured the quality of a control part printed using FDM and photopolymer jetting. Feature completion and dimensional accuracy were the main measures of part quality. They measured the smallest gap width of a printed slot feature and determined that the minimum resolution of the studied machines varied from 0.4 to 0.6 mm. Upcraft and Fletcher [9] analyzed the dimensional accuracy of several AM techniques, including FDM. They found that none of the processes were capable of achieving dimensional accuracy greater than 97.8%.

Other studies have developed techniques to improve the accuracy of FDM. One example of error compensation is the use of an optimal shrinkage compensation factor (SCF) [10,11]. A disadvantage of the SCF is that only one compensation factor is used for all directions and it only applies for homogeneous deviations.

Any approach to improve the accuracy of FDM must be based on a reliable characterization of error in the process. Thus, the goal of this paper is to identify process- and machine-related error sources in FDM so that a framework that characterizes error in an FDM machine may be developed using an error budget approach.

IDENTIFYING ERROR SOURCES IN FDM

This research first examined how the build orientation and part density affected the form and resolution of FDM parts. Six control parts (Figure 1) were manufactured on two FDM machines: Stratasys Dimension BST 1200es and SST 1200es. These FDM machines have a minimum layer thickness of 0.254 mm and produce parts made from "ABS*plus,*" which has similar mechanical properties to acrylonitrile butadiene styrene (ABS) [12]. The control parts were printed with two different density settings from each machine: solid and low density. All other parameters were kept constant.

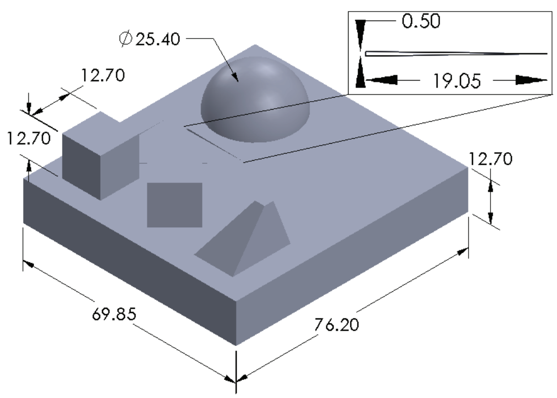

FIGURE 1. Control part #1 used to quantify form errors and resolution in FDM (all units in [mm]).

An Olympus SZ optical microscope was used to measure the form and resolution of the control part. Form was evaluated using the measured roundness of the hemisphere feature and qualitative observations of the printed part. Resolution was estimated from the length and minimum width of the tear drop feature.

To investigate the influence of the staircase effect on the surface roughness, another control part (Figure 2) was designed with surfaces that varied the build orientation (θ) from $0° \le \theta \le 90°$ in intervals of 5°. The surface roughness R_a of each surface was measured using a MarSurf M1 stylus tip profilometer along the measurement path delineated in Figure 2. This profilometer had a tip radius of 2.5 μm and profile resolution of 12 nm.

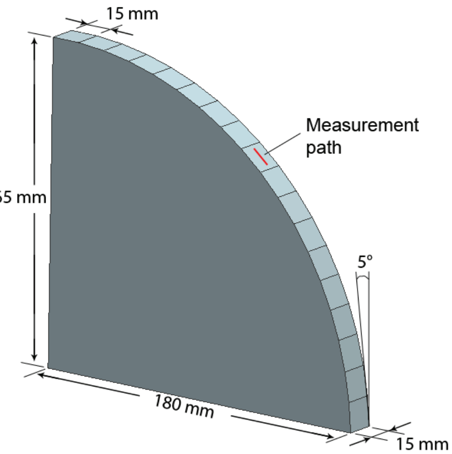

FIGURE 2. Control part #2 used to investigate the staircase effect on surface roughness.

To quantify accuracy and precision across the entire work volume, the control part shown in Figure 3 was printed on the Stratasys Dimension SST 1200es. This control part was measured with a coordinate measuring machine with a scanning head of 6 mm diameter. The actual position of each corner point was identified as the intersection of the three adjoining planes, which were located by approximating best-fit planes using ~400 measured points on each surface. The root mean square (RMS) deviation between the actual and nominal position of each corner point represented the accuracy at each position in a specific direction (Equation 1). The precision was represented by the extended interquartile range IQR_{ext}, which contained 90% of all measurement points at a specific position.

$$RMS_x = \sqrt{\frac{\left(x_1^{act}-x_1^{nom}\right)^2+\cdots+\left(x_n^{act}-x_n^{nom}\right)^2}{n}} \quad (1)$$

Results

Figure 4 shows the observed form error in control part #1 (Figure 1); it indicates gaps where material was not deposited. Roundness was estimated by examining the second deposition layer from the top of the hemisphere and drawing the smallest circle that would enclose the layer and the largest circle that would reside within the layer. The difference between the two radii was calculated and is shown in Table 1.

The resolution was estimated by first identifying the tip of the printed tear drop feature. The length of the tear drop features was significantly smaller than the desired length: the average length was 13.9 mm versus the average desired length of 19.1 mm. The expected width of the tear drop feature at its printed tip was then used as the resolution estimate. Table 2 shows the calculated average minimum resolution in the *x*, *y*, and *xy* directions for both FDM machines studied in this paper.

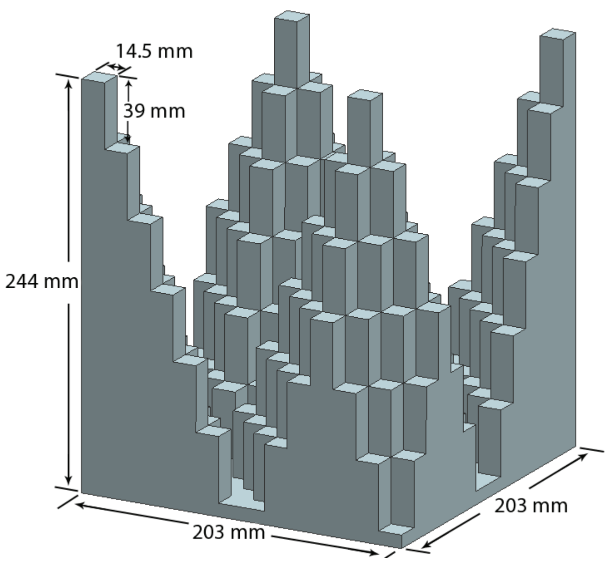

FIGURE 1. Control part #3 used to estimate the accuracy and precision of FDM.

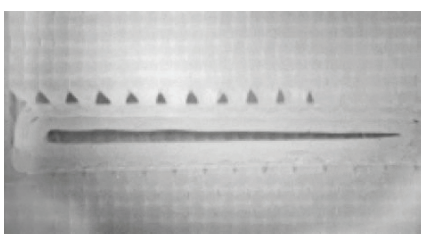

FIGURE 4. Form error observed in control part #1.

TABLE 1. Roundness error of the SST and BST control parts [mm].

Machine	Density	Radius Difference [mm]
SST	Solid	0.272
SST	Low	0.215
BST	Solid	0.438
BST	Low	0.313

Figure 5 shows the surface roughness of each face measured on control part #2. It illustrates the anticipated increase in surface quality that occurs when the build orientation increases over the range 45° ≤ θ ≤ 90°.

TABLE 2. Average minimum resolution of the SST and BST control parts [mm].

Machine	Density	Avg Min Resolution [mm]
SST	Solid	0.143
SST	Low	0.130
BST	Solid	0.128
BST	Low	0.126

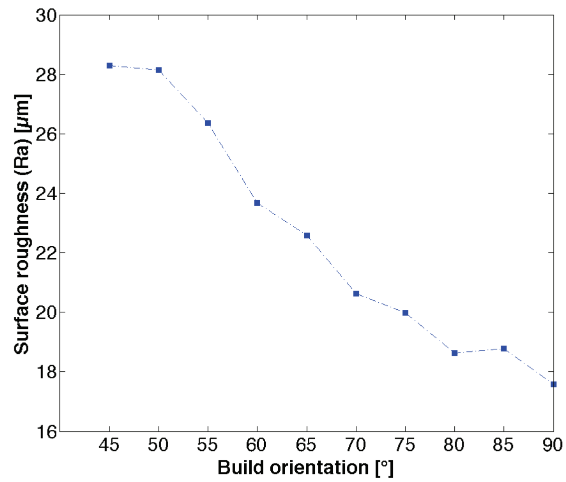

FIGURE 5. The relationship between surface roughness and build orientation for control part #2.

Table 4 shows the estimated accuracy based on the measurement of control part #3. Accuracy with respect to the *y* direction is greater than that with respect to the *x* direction. This could have been caused by the axis configuration. Since the *y* axis carries the *x* axis, the error in the *x* direction could have been additionally influenced by the error in the *y* axis.

TABLE 3. Comparison of achievable accuracy for deviations in x, y, and z directions.

Direction	Lower Limit	Upper Limit
x	0.12 mm	0.62 mm
y	0.08 mm	0.30 mm
z	0.21 mm	0.57 mm

Table 4 summarizes the estimated precision based on the measurement of control part #3 for the *x*, *y*, and *z* directions, respectively, with respect to different positions. Generally, the z direction has the greatest precision for the FDM machine in this study.

TABLE 4. Comparions of precision in the x, y, and z directions with respect to different x, y, and z positions.

	X Direction $IQR_{ext.}$[mm]		Y Direction $IQR_{ext.}$[mm]		Z Direction $IQR_{ext.}$[mm]	
	Min.	Max.	Min.	Max.	Min.	Max.
X Position	0.32	0.71	0.26	0.70	0.26	0.51
Y Position	0.21	0.89	0.12	0.59	0.17	0.41
Z Position	0.23	0.58	0.27	0.90	0.19	0.24

CHARACTERIZING ERROR IN FDM

The second part of this research focused on a framework to characterize and quantify error in the FDM process. This was completed by developing an error budget for the Stratasys Dimension SST 1200es.

The axis configuration of the considered FDM machine was described as *w-Z-f-Y-X-t*, where the identified machine components are the workpiece *w*, the *z* axis, the fixed machine foundation *f*, the tool *t*, the *x* axis, and the *y* axis, which is also based on the fixed machine foundation. The parametric error components of the three linear axes have to be included in the mathematical error model. Every linear axis had six component deviations (scale error, two straightness errors, role, pitch, and yaw) and three position deviations (deviation of the initial position and two squareness errors with respect to the other axes). Therefore, the total number of error components considered should have been 27 [13]. But, by defining the coordinate system of a machine tool, its zero position deviations and three of its squareness errors were set to zero. This meant that the FDM required 21 error components since it has three linear axes.

Homogeneous Transformation Matrices (HTMs) were used to transform the coordinates and errors of one component to the coordinate system of another component. Generating two HTMs that represented the location of the nozzle tip and a desired location on the workpiece, respectively, relative to the fixed machine foundation captured the influence of all error components with respect to the reference frame. The general HTM for the transformation of a linear axis with coordinate system *J* into coordinate system *I* is shown in Equation 2, where *δ* represents translational errors, *ε* represents rotational errors, and *a*, *b*, and *c* are offsets between the different coordinate systems in *x*, *y*, and *z* direction, respectively. The deviation between the nozzle tip and workpiece location was a measure of the process error.

$$T_{IJ} = \begin{bmatrix} 1 & -\epsilon_z(j) & \epsilon_y(j) & a_j + \delta_x(j) \\ \epsilon_z(j) & 1 & -\epsilon_x(j) & b_j + \delta_y(j) \\ -\epsilon_y(j) & \epsilon_x(j) & 1 & c_j + \delta_z(j) \\ 0 & 0 & 0 & 1 \end{bmatrix} \quad (2)$$

Because the FDM machines used in this study provided less direct control of each axis, the use of standard experiments to determine the error components was not feasible. Instead, each error component was approximated using a Legendre polynomial P^i (Equation 3) [14]. Thus, approximating error component required calculating the polynomial coefficients a_i. But, this approximation makes it impossible to differentiate between the scale and squareness errors of an axis. Therefore, the FDM machine was assumed to be an orthogonal system [15], and the number of considered error components was reduced to 18.

$$\delta_x(x) = \sum_{i=0}^{n} a_i \cdot P^i(x) \quad (3)$$

The mathematical model was implemented as a least squares problem in MATLAB®. This approach required data from a minimum of 54 features to determine 21 error components with three polynomial coefficients each (this was the motivation for the design of control part #3). The number of features actually generated in control part #3 was greater than the minimum needed, though, to create an overdetermined system of equations that would have minimized the influence of nonrepeatable error terms and allow for a more accurate approximation of the error components. In addition to the error components, the error gains (or offsets between the origins of each component coordinate system) were measured.

Results

The results of the error budget demonstrate the approximated propagation of the translational and rotational error components of each linear axis. Selected results are shown in Figures 6, which display the translational error components of the *y* axis. Generally, it was determined that third order Legendre polynomials, which have been used primarily in literature [16,17], have greater approximation error than second order Legendre polynomials.

By using the second order approximation, it was determined that among the translational error components, the main contributors to the error of the machine tool are: the straightness error of the *x* axis in the *z* direction, the straightness error of the *y* axis in the *x* direction, and the straightness error of the *y* axis in the *z* direction, with maximal values in the range of 0.011 - 0.014 mm. The scale errors of the three axes were investigated to be less. Among the rotational error components, it was identified that the yaw of the *z* axis with a maximal value of ~600 arc seconds is the main contributor to the overall machine error. Thus, the rotational errors of the *x* and *y* axes could be neglected during first improvement attempts.

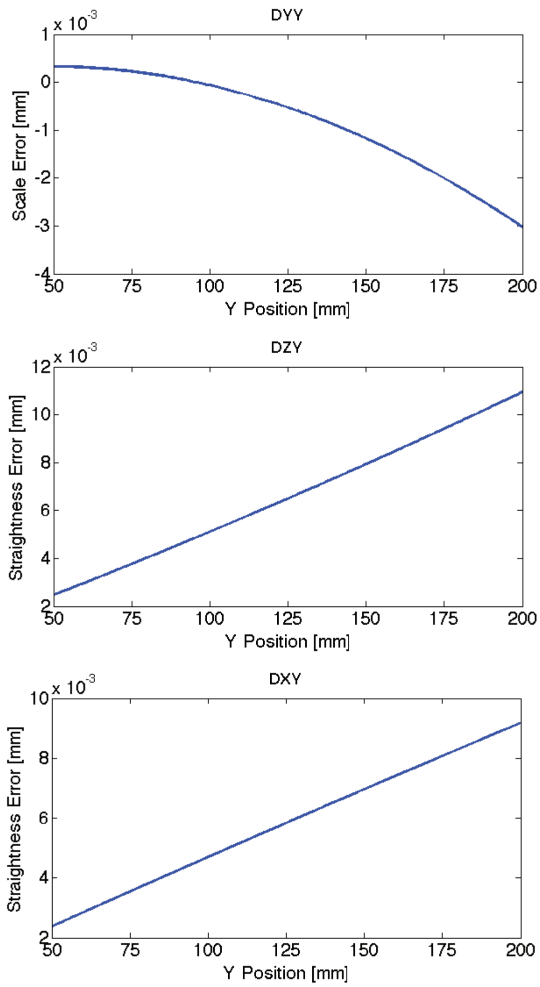

FIGURE 6. Approximated translational error components of the y axis.

CONCLUSION AND FUTURE WORK

The goal of this paper was to understand how process characteristics influenced error generation in FDM. Different sources of error were identified by focusing on the effect of build orientation and part density on form, resolution, and surface roughness. Control parts were utilized to quantify these errors. Accuracy and precision were estimated across a large portion of the work volume, and these results informed the development of an error budget framework for FDM that can help characterize the error expected in the process.

The presented work did have some limitations that should be addressed in future work. For example, control part #1 did not cover the entire printable area of the machine, which means that some of the observed errors could have been different if the control part were located on a different part of the printing bed. Also, determining the overall accuracy and precision for the examined FDM machine tool was not possible. The common procedure to determine each error component was not feasible due to limited control of axis motion and process parameters as well as an inability to clamp measurement equipment to the FDM machine. Thus, the component errors could only be approximated. Additional sources of error could have also existed that contributed nonrepeatable errors that were assumed to be zero in the error model. Finally, material behavior was a major error source that was not considered because of its unclear impact on the error budget. Therefore, the results presented likely had some modeling error.

Future work will seek to use FDM machines that provide control of additional process parameters. Furthermore, the accuracy of approximations using the error budget will be improved by considering additional sources of error since the current model only considers the component deviations of the machine tool as sources of error. Process errors and errors caused by material behavior will also be considered since they are expected to be significant. Finally, further validation of the approximated error components in this study will be conducted to better quantify modeling error.

The work presented in this paper illustrates the current limitations of FDM by contributing to an understanding of error generation. The results of this work can be used to identify possible process improvements in the design and control of FDM technology. Ultimately, these types of innovations are necessary for AM to be more widely accepted in industry.

ACKNOWLEDGEMENTS

The authors would like to acknowledge the helpful contributions of WooJung Choi and Abhishek Khemka. They would also like to thank

Scott McCormick, Gordon Long, and Robert Connors for their valuable assistance and guidance with this research.

REFERENCES

[1] Bourell D, Leu M, Rosen D. Roadmap for Additive Manufacturing - Identifying the Future of Freeform Processing. The University of Texas at Austin Laboratory for Freeform Fabrication Advanced Manufacturing Center. 2009.

[2] Levy G, Schindel R, Kruth J-P. Rapid Manufacturing and Rapid Tooling with Layer Manufacturing (LM) Technologies, State of the Art and Future Perspectives. CIRP Annals – Manufacturing Technology 52. 2003; 2: 589-609.

[3] Sood A, Ohdar R, Mahapatra S. Improving Dimensional Accuracy of Fused Deposition Modeling Processed Part Using Grey Taguchi Method. Materials & Design 30. 2009.

[4] Kruth, J. Material Incress Manufacturing by Rapid Prototyping Techniques. CIRP Annals - Manufacturing Technology 40. 1991; 2: 603–614.

[5] Hackney P. An Investigation into the Characteristics of Materials and Processes, for the Production of Accurate Direct Parts and Tools using 3D Rapid Prototyping Technologies. Doctoral Thesis, Northumbria University. 2006.

[6] Masood S.H, Rattanawong W, Iovenitti P. Part Build Orientations Based on Volumetric Error in Fused Deposition Modelling. The International Journal of Advanced Manufacturing Technology, February 2000, Volume 16, Issue 3, pp 162-168.

[7] Ahn D, Kweon J, Kwon S, Song J, Lee S. Representation of Surface Roughness in Fused Deposition Modeling. Journal of Materials Processing Technology, May 2009.

[8] Clemon L, Sudradjat A, Jaquez M, Krishna A, Rammah M, Dornfeld D. Precision and Energy Usage for Additive Manufacturing. Proceedings of the ASME 2013 International Mechanical Engineering Congress & Exposition. November 13-21, 2013.

[9] Upcraft S, and Fletcher R. The Rapid Prototyping Technologies. Assembly Automation 23. Dec. 2003; 4: 318–330.

[10] Dao Q, Frimodig J C, Le H N, Li X-Z, Putnam S B, Golda K, Foyos J, Noorani R, and Fritz B. Calculation of Shrinkage Compensation Factors for Rapid Prototyping (FDM 1650). Computer Applications in Engineering Education 7. 1999; 3: 186–195.

[11] Gregorian A, Elliot B, Navarro R, Ochoa F, Singh H, Monge E, Foyos J, Noorani R, Fritz B, and Jayanthi S. Accuracy Improvement in Rapid Prototyping Machine (FDM-1650). In Solid Freeform Fabrication Proceedings. 2001; 77–84.

[12] Stratasys Ltd. Web. 12. March. 2014. http://www.stratasys.com/3d-printers/design-series/performance/dimension-1200es

[13] Okafor A, Ertekin Y M. Derivation of Machine Tool Error Models and Error Compensation Procedure for Three Axes Vertical Machining Center using Rigid Body Kinematics. International Journal of Machine Tools and Manufacturing 40. 2000; 8:1199-1213.

[14] Tong K, Joshi S, and Lehtihet E A. Error Compensation for Fused Deposition Modeling (FDM) Machine by Correcting Slice Files. Rapid Prototyping Journal 14. Jan. 2008; 1: 4–14.

[15] Tong K, Lehtihet E, Joshi S. Parametric Error Modeling and Software Error Compensation for Rapid Prototyping. Rapid Prototyping Journal 9. 2003; 4: 301-313.

[16] Kruth J, Vanherck P, and De Jonge L. Self-calibration Method and Software Error Correction for Three-dimensional Coordinate Measuring Machines using Artefact Measurements. Measurement 14. Dec. 1994; 2: 157-167.

[17] Tan K K, and Hang S. Geometrical Error Compensation of Machines with Significant Random Errors. ISA Transactions 44. Jan. 2005; 1: 43-53.